Vietnam Journal of Catalysis and Adsorption
Tạp chí xúc tác và hấp phụ Việt Nam

https://chemeng.hust.edu.vn/jca/

Resorcinol Formaldehyde Resin-Modified Carbon Nitride as Metal-free Photocatalyst for Water Treatment

Tran Hong Minh[1], Nguyen Xuan Truong[1] , Nguyen Ngoc Tue[1], Nguyen Duc Trung[1], Giang Thi Phuong Ly[1], Tran Thuong Quang[1*]

[1] *School of Chemical Engineering, Hanoi University of Science and Technology, Hanoi, VIETNAM*
**Email: quang.tranthuong@hust.edu.vn*

ARTICLE INFO

Received: 10/5/2022
Accepted: 15/6/2022
Published: 20/6/2022

Keywords:

Resorcinol-Formaldehyde Resin, Carbon Nitride, Photocatalyst, Methylene Blue

ABSTRACT

Metal-free catalysts are considered a new strategy for environmental application since they do not release any additional hazardous compounds when employed for an extended period. Carbon-based materials and carbon nitride have drawn a lot of interest owing to their physical and optical properties. Herein, we reported a new way to modify carbon nitride with resorcinol-formaldehyde resins, a member of phenolic resins, to enhance their photocatalytic activity. The length of time to polymerize resorcinol-formaldehyde resins was investigated as it had a great impact on the characteristic features as well as the photocatalytic performance of the resulting materials. SEM images revealed that RF resins appeared as nano-fragments and were deposited densely on the surface of carbon nitride. On the other hand, the deposition of RF on the surface of carbon nitride had a great influence on the BET surface area values. For photocatalytic performance, all the modified samples exhibited significantly improved photocatalytic activity towards Methylene Blue (MB). The optimal sample was RF@CN10, which the reflux time was 10 hours. This sample has a more broaden absorption spectrum and a narrower bandgap energy (2.66 eV) than the pure carbon nitride. With regard to photocatalytic activity, this sample could completely degrade MB in the solution within 40 minutes, but it had poor efficiency when visible light was absent. Additionally, the catalyst could work effectively in neutral and alkaline conditions and could be reused for 5 cycles. Finally, the hypothesis for RF-carbon nitride cross-linking and the synergistic effect in the catalyst had been proposed.

Introduction

Metal-free photocatalysts for water treatment are considered a sustainable strategy to tackle various environmental problems. They have comparable or even greater photocatalytic activity than metal-containing photocatalysts, including tunable structure, visible light response, good electrical conductivity, and thermal and chemical stability. While metal-derived photocatalysts are harmful due to metal ion leakage

https://doi.org/10.51316/jca.2023.004

into the environment, metal-free materials can be exceedingly stable and non-toxic. Earth-abundant elements including carbon, nitrogen, oxygen, and semiconductor elements (e.g. Si, Se, P, S, B, Te) make up the majority of metal-free photocatalysts [1]. Some typical applications of metal-free photocatalysts are water splitting, CO_2 reduction, decomposition of organic pollutants, water disinfection, and microbial control. In this study, two types of materials will be discussed in detail, including graphitic carbon nitride (g-C_3N_4) and Resorcinol formaldehyde resin (RF).

Graphitic carbon nitride (g-C_3N_4), a class of metal-free materials, has drawn great attention from many researchers recently. In terms of morphology, carbon nitride has a similar layered structure to graphene, with triazine and tri-s-triazin units forming each layer [2]. In certain aspects, carbon nitride outperforms graphene due to the abundance of nitrogen atoms in the material. Owing to its fascinating properties such as narrow bandgap energy (~2.7eV), visible light response, stability, carbon nitride has been proposed as a promising candidate for environmental application [3]. In the year 2009, Wang et al reported that carbon nitride could split water to produce H_2 and O_2 under visible light, starting a significant development of this promising photocatalyst [4]. Carbon nitride and its derivatives are currently investigated in various fields of application ranging from water purification [5,6], CO_2 reduction [7], sterilization [8], energy storage [9].

Resorcinol formaldehyde resins, a member of the class of phenolic resins, are synthesized from the polycondensation of resorcinol and formaldehyde. Because they can form strong bindings that are resistant to moisture, acids, and weathering, they are mostly used as adhesives in many industrial production processes [10]. Recently, RF has emerged as a potential material that can be used to prepare nanostructured carbons for various applications, such as adsorbents, battery electrodes, super-capacitors, drug delivery carriers, and catalytic supports. Previous literature had reported that RF resin itself had catalytic activity owing to its intriguing structure that consists of π-stacking of the benzenoid–quinoid couples [11]. RF-derived materials also have a large surface area and porous structure, making them suitable adsorption applications.

Another significant feature of RF resins is their adjustable structure. Many groups reported that the physicochemical properties and function of RF resins can be varied by introducing hetero elements such as nitrogen [6], sulfur [12], or inorganic nanoparticles. The Stöber method consider as the classic method to prepare RF nanostructures [13].

In this research, we had successfully prepared a series of RF-carbon nitride composites for photocatalyst application. The modification of carbon nitride with RF resins aimed to enhance physical characteristics and photocatalytic activity toward organic pollutants, such as methylene blue. XRD, FTIR, SEM, and N_2 adsorption-desorption isotherms were used to characterize the as-prepared composite materials. The photocatalytic performance of the as-prepared composites was evaluated by Methylene blue (MB) degradation reaction under visible light irradiation in room condition. Several reaction parameters, such as the presence of visible light, the pH solution, and the doses used for a single reaction, were also investigated.

Experimental

Materials and substances

All chemicals and compounds were bought from commercial providers and utilized without additional purification. Urea (>99%, Xilong, China), Resorcinol (>99%, Xilong, China), Formaldehyde solution (37-40%, Xilong, China), Dimethylformamide (DMF, >99%, Xilong, China), Ammonia solution (25-28%, Xilong, China), Methylene Blue (MB, >99%, Xilong, China), Hydrochloric acid (HCl, 36-38%, Xilong, China), Sodium hydroxide (NaOH, >96%, Xilong, China), Methanol (CH_3OH, >99%, Xilong, China). Distilled water from our laboratory was used for all test experiments.

Preparation of g-C_3N_4

Carbon nitride (g-C_3N_4) was prepared via thermal polycondensation, with urea as the precursor. In brief, 50 g of urea was heated to 550° in static air at a ramp rate of 2°C/min, and kept at this temperature for 3h. After the thermal condensation, the sample was cooled naturally to room temperature before being used for the preparation of RF-carbon nitride composites. The obtained light-yellow solid was also denoted as CN.

Preparation of RF@CN

RF@CN samples were synthesized by solvothermal reflux method. At the beginning of the synthesis process, Resorcinol (400 mg, 3.6 mmol), NaOH (concentration 1M, 1ml), and formaldehyde (480 μl, 7.2 mmol) were dissolved in 25 ml DMF solvent, which was previously placed in a 250-ml two-neck round-bottom

flask. Then 1 g of CN sample was suspended into the mixture by magnetic stirring. From there, the flask was attached to the reflux condenser and heated up to 120°C. The temperature was kept constantly for x hours (x (h)= 6, 10, and 19). After refluxing in alkaline condition, HCl acid was put into the flask until the mixture was acidic (pH~3), then the mixture continued refluxing for another hour. Next, the flask was left to cool down to room temperature, and the light orange solid was collected by vacuum filtration. Following that, the solid sample was washed with water and methanol several times, and eventually dried at 80°C for 24h. The final products were denoted as RF@CNx.

Characterization

A Bruker D8 Discovery X-ray Diffractometer was used to produce XRD patterns using Ni-filtered Cu-K radiation (λ = 0.154056 nm) as the X-ray source. The recorded range of 2θ was from 5° to 45° and the scanning rate was set at 4° per min. The FTIR spectra were obtained at room temperature using a JASCO FT/IR6300 Spectrometric Analyzer in the 400 to 4000 cm^{-1} range. Field-emission scanning electron microscopy (FESEM) measurements were performed on a JSM-7800F Prime scanning electron microscope to study the morphology of the samples. The Brunauer–Emmett–Teller (BET) surface areas and pore size distribution of the samples were measured using the nitrogen adsorption isotherm on a Gemini VII 2390 V1.02 surface area analyzer at 77 K.

Catalytic degradation experiments

Methylene Blue (MB) degradation experiments were conducted under visible light irradiation. The visible light was generated by a high-pressure Mercury lamp 250W, from OSRAM. In brief, 20 mg of sample was suspended into 50 mL of 10 mg L^{-1} MB aqueous solution under stirring process by magnetic stir at ambient conditions. The mixture was then placed under the light sources. Every 10 minutes, the residual dye concentration in centrifugal fluid was evaluated using a Hatch UV–vis spectrophotometer model DR 3900 with a 1 cm quartz cell at the maximum wavelengths of MB (664 nm).

To determine the stability of RF@CN samples, the residual catalyst was recovered from the resulting MB aqueous by centrifugation and reused for subsequent reactions.

Results and discussion

Characterization of the prepared RF@CN

To analyze the structural phases of all samples, the X-ray Diffraction technique was used, and the recorded spectra are presented in Figure 1a. Looking at the pattern of pure carbon nitride, a sharp signal at around 27.6° reflected the interplanar stacking of the conjugated aromatic systems with an interplanar distance d = 0.322 nm, while a weak one at around 13° was characteristic of the in-plane structural packing motif. These characteristic diffractions were in good agreement with previous reports for carbon nitride [14,15]. For XRD patterns of RF-modified carbon nitride, no strange reflexes were observed, owing to the similarity in the lattice structure between RF resins and carbon nitride. However, the intensity of the diffraction band at round 13° increased slightly when lengthening the polymerization step, indicating that more RF resins cling to carbon nitride's surface.

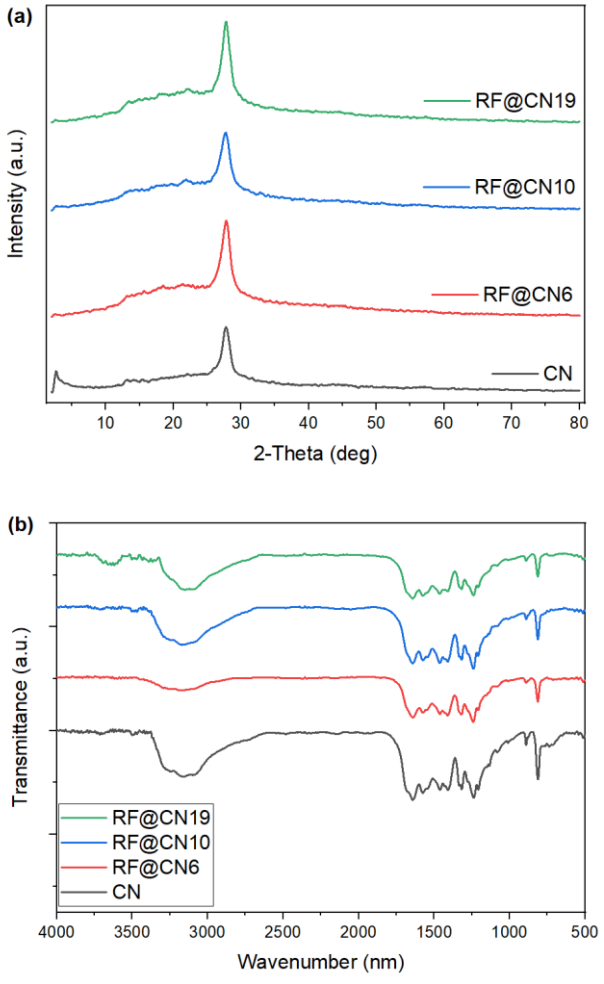

Figure 1: XRD patterns (a) and FTIR spectra (b) of Carbon nitride and RF@CN samples

The functional groups present in carbon nitride and RF@CN samples were examined by FTIR method and shown in Figure 1b. The black curve of pure carbon nitride exhibited various characteristic absorption peaks, which matched well with previous reports [16,17]. In the region of 1200-1600 cm^{-1}, two absorption peaks at 1641 and 1576 cm^{-1} were attributed to stretching vibration of C=N, while three peaks at 1462, 1317, and 1238 cm^{-1} corresponded to C–N of the heterocycles. Additionally, a strong peak recorded at 812 cm^{-1} was assigned to the breathing mode of s-triazine units of carbon nitride layers. It can be seen that FTIR spectra of pure carbon nitride and RF@CN sample were almost identical, except for the reduction of the feature for the breathing mode of s-triazine units.

Table 1: BET surface area of CN and RF@CN samples

Samples	BET surface area [a] (m^2 g^{-1})	Pore volume [b] (cm^3 g^{-1})	Pore size [c] (Å)
CN	102.4323	1.859212	644.993
RF@CN6	17.1767	0.527316	1133.624
RF@CN10	32.9830	0.262155	303.951
RF@CN19	27.2562	0.225293	301.684

[a] BET specific surface;
[b] Pore volume calculated from the adsorption branch of the isotherm using the BJH method.
[c] Pore size calculated from the adsorption branch of the isotherm using the BJH method.

The measurement of nitrogen adsorption-desorption isotherms was used to evaluate the porous properties and specific surface area of CN and RF@CN samples, and the BET surface area results are depicted in Table 1 and Figure 2. From Table 1, BET surface area of CN sample was 102.43 m^2 g^{-1}, which is surprisingly higher than previous studies on carbon nitride [17]. Meanwhile, the values for RF@CN samples were in the range from 17 m^2 g^{-1} to 33 m^2 g^{-1}, significantly smaller than that of the pure CN due to the presence of RF resins. The RF@CN6 sample has the lowest surface area value that can be explained due to the small size of RF fragments that made it easier for these fragments to anchor in the pores of carbon nitride.

UV-Vis DRS was used to study the optical properties of the samples. Figure 3a is plotted UV-Vis DRS spectra of pure carbon nitride and RF@CN10. Looking at the black line, it is clear that pure carbon nitride had an optical absorption range between 200 and 450 nm, which is consistent with previous research results on carbon nitride materials. Meanwhile, the RF@CN10 sample is able to absorb light in the region with wavelength higher than 450 nm. This can be explained that modifying carbon nitride with RF polymer fragments may enhance light absorption properties of the sample. In terms of bandgap energy (Figure 3b), pure carbon nitride has a higher value (2.86 eV) than the RF@CN10 (2.66 eV).

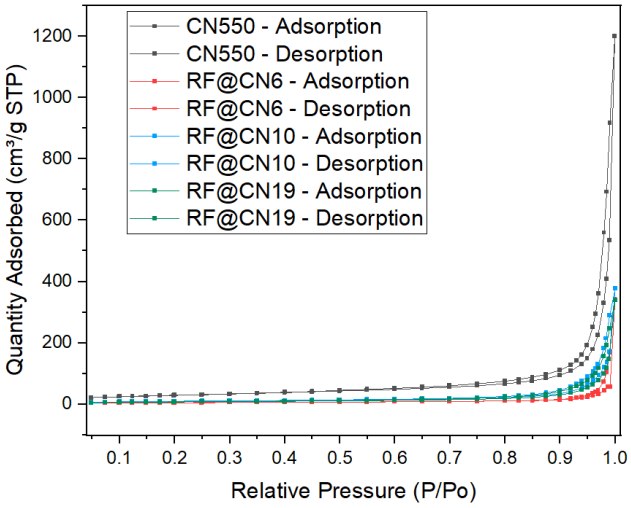

Figure 2: Nitrogen adsorption–desorption isotherms of CN and RF@CN samples

The morphology of pure carbon nitride and the RF-modified sample could be observed in SEM images presented in Figure 4. It can be seen from Figure 4ab that pure carbon nitride's morphology was made up of layers orderly stacking on each other [15]. As can be seen from Figures 4cd, RF@CN10 had a stacking-fragment structure.

Additionally, these uneven nano-sized fragments can be assigned to RF resins modified on the surface of carbon nitride. These RF resin fragments were deposited densely, thus reducing the pores size of the composite material. These changes in morphology corresponded to the changes in XRD patterns and BET surface area values presented in the previous part of this study.

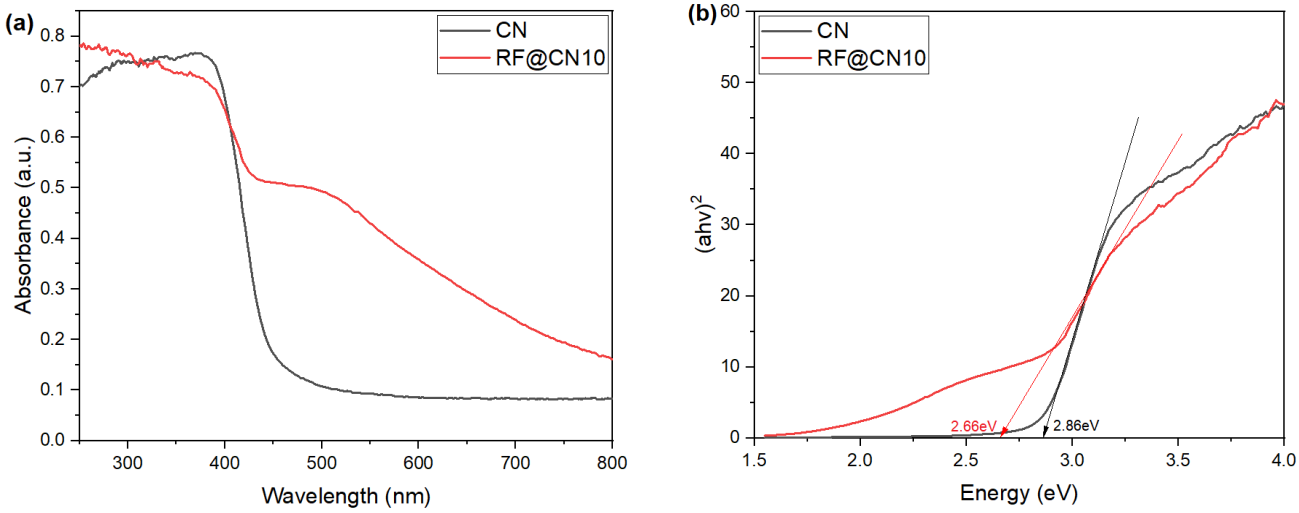

Figure 3: (a) UV-vis DRS spectra and (b) calculated band gap of CN and RF@CN10

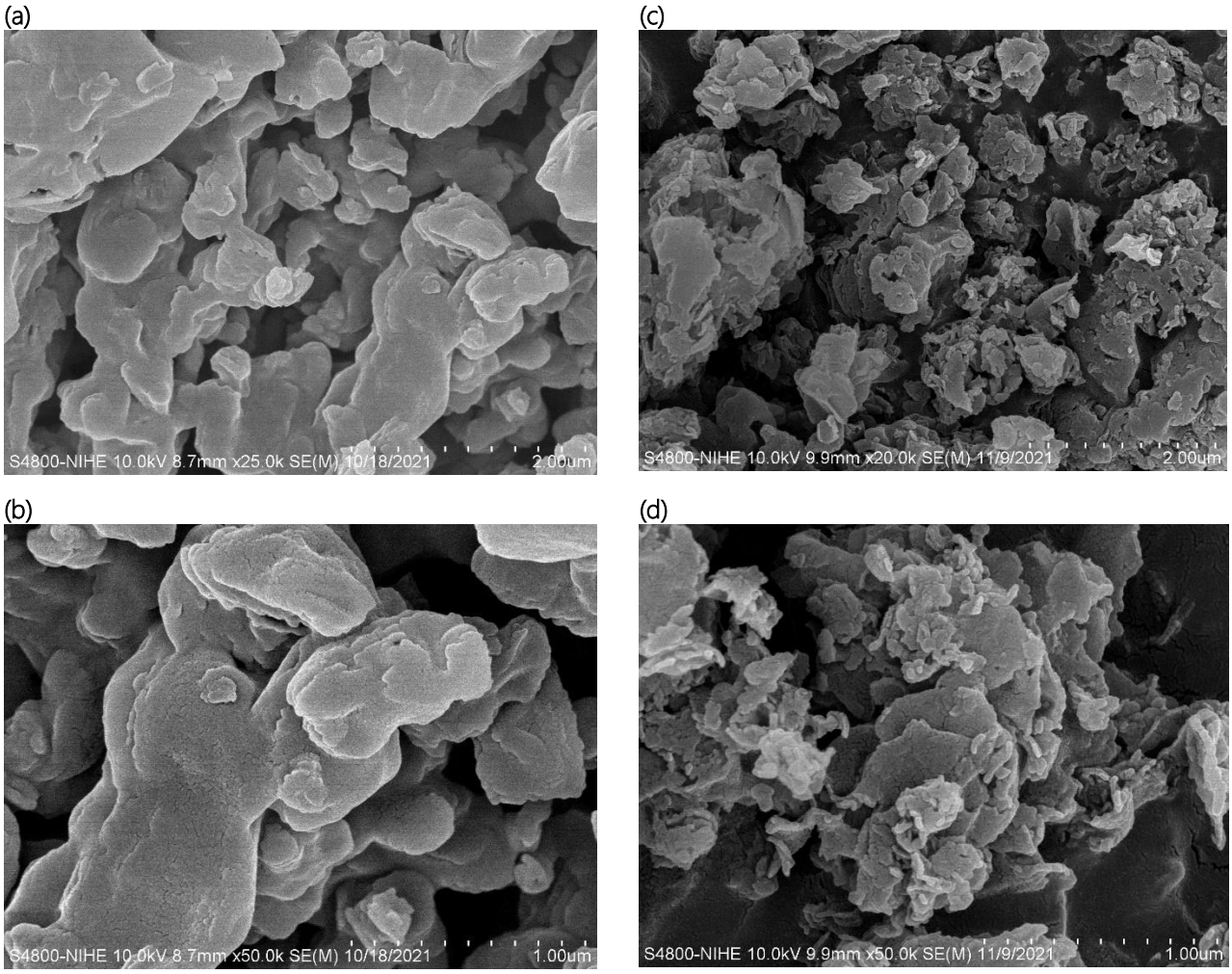

Figure 4: SEM images of (a,b) pure carbon nitride and (c,d) RF@CN10

https://doi.org/10.51316/jca.2023.004

The photocatalytic activity analyses

To evaluate the catalytic performance of RF@CN samples, various MB degradation experiments were conducted in ambiance conditions along with visible light irradiation. The results are plotted in Figure 5. Looking at the pattern of CN550, only 20% of MB was removed within 70 minutes. By contrast, all RF-modified carbon nitride samples outperformed the pristine CN. It can be seen from Figure 5 is that RF@CN6 could remove 97% of MB within 70 minutes, the slowest among three RF@CN samples. The optimal sample is RF@CN10, with the degradation efficiency being at nearly 100% within 40 minutes under visible light irradiation. The degradation performance of RF@CN19 was 100% within 60 minutes, indicating that the longer polymerization of RF resins could reduce the catalytic performance of RF@CN composite. Compared to other metal-free catalysts in Table 2, RF@CN composite exhibited good physical properties as well as excellent photocatalytic activity.

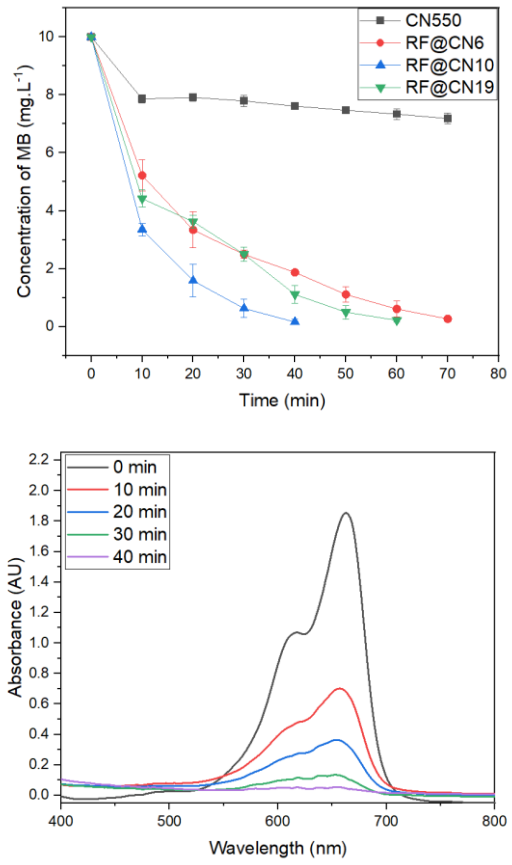

Figure 5: (a) Effects of solvothermal time on the catalytic performance of RF@CN samples; Error bars represent one standard deviation for three measurements. (b) UV-vis spectra during catalytic reactions (λ_{max}=664 nm).

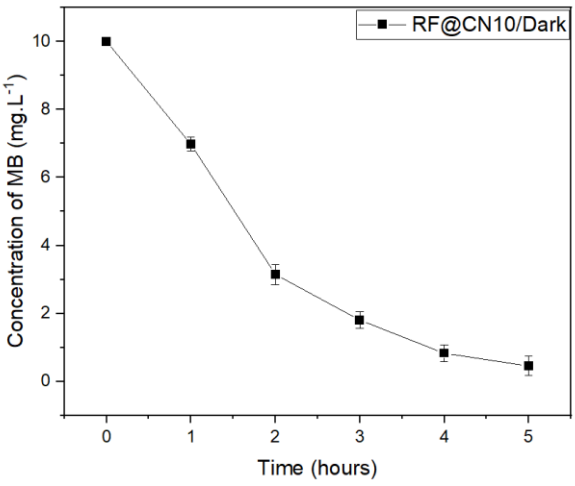

Firgure 6: Removal of MB without visible light; Error bars represent one standard deviation for three measurements. (Experimental conditions: MB, 10mg L^{-1}; pH 5-7, and catalyst, 0.4 g L^{-1})

The ability to remove MB of the RF@CN10 sample was further investigated by conducting experiments in the absence of light. It can be seen from Fig 6 that RF@CN10 could remove all the MB within 5 hours without visible light irradiation. The results proved that RF@CN10 had superior performance when exposed to visible light, confirming the photocatalytic activity of RF@CN samples.

pH of the solution is a crucial parameter that can affect the photocatalytic process dramatically. Therefore, the effect of pH was thoroughly evaluated by varying the initial pH value of MB solution from 3 to 9 using 0.1 M NaOH solution and 0.1 M HCl solution. The results are presented in Figure 7.

In the acidic environment, the catalyst's performance reduced greatly. To be more specific, in pH 3, MB was completely decomposed within 140 minutes under visible light, compared to 100 minutes in the pH 5 condition. From Figure 7, it is noticeable that the dye degradation efficiency of RF@CN in alkaline medium and strong conditions were much better. In pH 7 and above, RF@CN10 could completely remove MB in the solution within 40 minutes. It could be explained that RF@CN could produce more reactive species (e.g superoxide radicals) in alkaline conditions, thus enhancing the MB degradation efficiency. This phenomenon has been reported in previous research about carbon nitride [16].

https://doi.org/10.51316/jca.2023.004

Table 2: Physical properties and photocatalytic performance of some metal-free photocatalysts

No	Photocatalyst (mg)	Band gap (eV)	S_{BET} (m^2 g^{-1})	Photodegradation experiments			
				Light source (W)	Pollutant (mg L^{-1})	Degradation rate (time min)	Ref
1	3D macroporous g-C_3N_4 (70)	1.98	24.6	Xenon lamp (300)	RhB (10)	100% (40)	[18]
2	PANI/g-C_3N_4 (100)	-	-	Xenon lamp (500)	MB (10)	92.8% (120)	[19]
3	g-C_3N_4-PANI-PPy (15)	-	-	Xenon lamp	MB (5 × 10^{-5} M)	100% (70)	[20]
4	g-C_3N_4 (50)	-	66.1	Xenon lamp (250)	MB (20)	100% (90) (with H_2O_2 support)	[17]
5	RF14 (2)	1.90	148.0	Iron-doped metal halide Ultraviolet-Visible lamp (250W)	MB (100 μM)	100% (300)	[21]
6	RF@CN10 (20)	-	32.98	Mercury lamp (250W)	MB (10)	100% (40)	This study

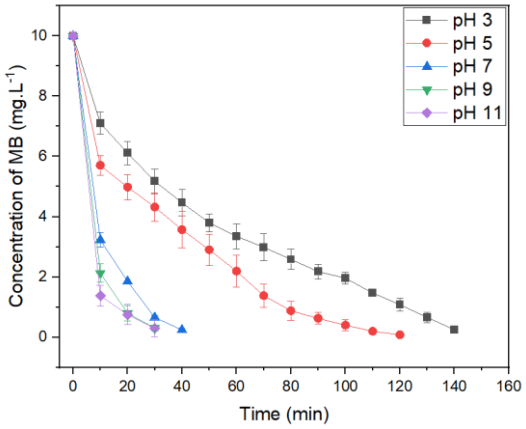

Firgure 7: Effect of initial pH on the degradation of MB; Error bars represent one standard deviation for three measurements (Experimental conditions: MB, 10mg L^{-1}; and catalyst, 0.4 g L^{-1})

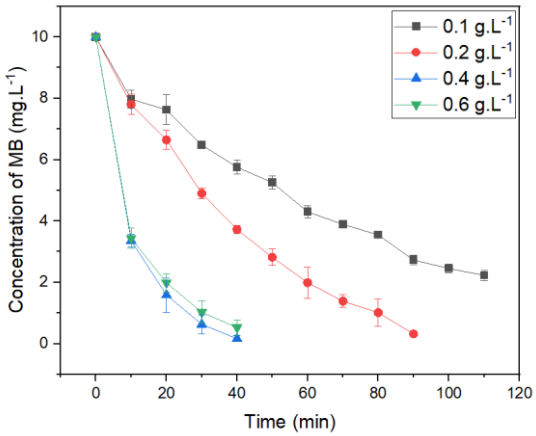

Firgure 8: Effect of catalyst concentration on the degradation of MB; Error bars represent one standard deviation for three measurements (Experimental conditions: MB, 10mg L^{-1}; pH natural)

In order to optimize the photocatalytic reaction, the effect of the catalyst dose on the MB treatment efficiency was investigated by running experiments over the Catalyst/Visible light/Natural pH system under ambiance conditions. The catalyst dose was varied from 0.1 g L^{-1} to 0.6 g L^{-1}, corresponding to the amount of solid catalyst from 5 mg to 30 mg. The experimental results are presented in Figure 8. As the amount of catalyst increased gradually from 0.1 g L^{-1} to 0.4 g L^{-1}, MB degradation efficiency increased gradually. When the catalyst dose was 0.1 g L^{-1}, MB treatment efficiency reached 71% after 90 minutes, compared to 98% in the equivalent time when the catalyst dose was 0.2 g L^{-1}. However, when increasing the catalyst dose from 0.4 g L^{-1} to 0.6 g L^{-1}, the MB decomposition performance was almost unchanged. Therefore, the optimal dose of RF@CN catalyst was 0.4 g L^{-1}.

Finally, the reusability of RF@CN10 was studied by conducting repeatedly photocatalytic reactions under visible light irradiation, and the results are displayed in Figure 9. It is clear that RF@CN10 photocatalyst could remove MB in an aqueous solution for five consecutive cycles. The MB removal rate at the end of each cycle was around 90%. However, it can be seen from the chart is that RF@CN10 performance in the 4^{th} and 5^{th} cycles are not as stable as the previous cycles, suggesting that MB residuals in the pores of the material from previous cycles slightly affect the activity of the material. In the future, this issue will be continue studying to enhance and prolong the catalytic activity of the RF@CN materials.

https://doi.org/10.51316/jca.2023.004

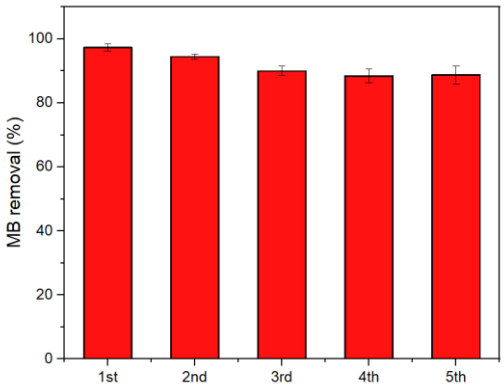

Figure 9: The reusability of RF@CN10 for MB photodegradation. Error bars represent one standard deviation for three measurements (Experimental conditions: MB, 10mg L^{-1}; catalyst, 0.4 g L^{-1}; pH natural; after 120 min irradiation for each time)

Catalytic mechanism of RF@CN composite

Previously studies on Carbon nitride have provided an overall photocatalytic mechanism of the degradation pollutants by this material [15]. Under visible light irradiation, electrons would be excited and moved to the conduction band (CB), creating photogenic holes (h+). Electrons would react with O_2 in solution to form Superoxide radicals ($\bullet O_2^-$). Meanwhile, the photogenic holes could participate in the reaction with H_2O or OH^- to generate hydroxy radicals (•OH). It is clear that •OH, $\bullet O_2^-$ and h+ are the main contributors to the photocatalytic process. As for resorcinol-formaldehyde resins, Shiraishi *et al* reported that RF resins contain a number of units consisting of electron acceptors (A) and electron donors (D), and this kind of A-D structure makes it possible for RF resins to function as semiconductors [11]. In addition, the π-stacking interaction of the couples creates the high conductivity properties of RF resins. By modifying RF resins on carbon nitride, the photocatalytic catalytic of the material had increased significantly, as shown in Figure 5. Thereby, we proposed a photocatalytic mechanism in Figure 10a. Owing to good conductivity, excited electrons could localize in the structure of RF resins, thus limiting the recombination of electrons and photogenic holes.

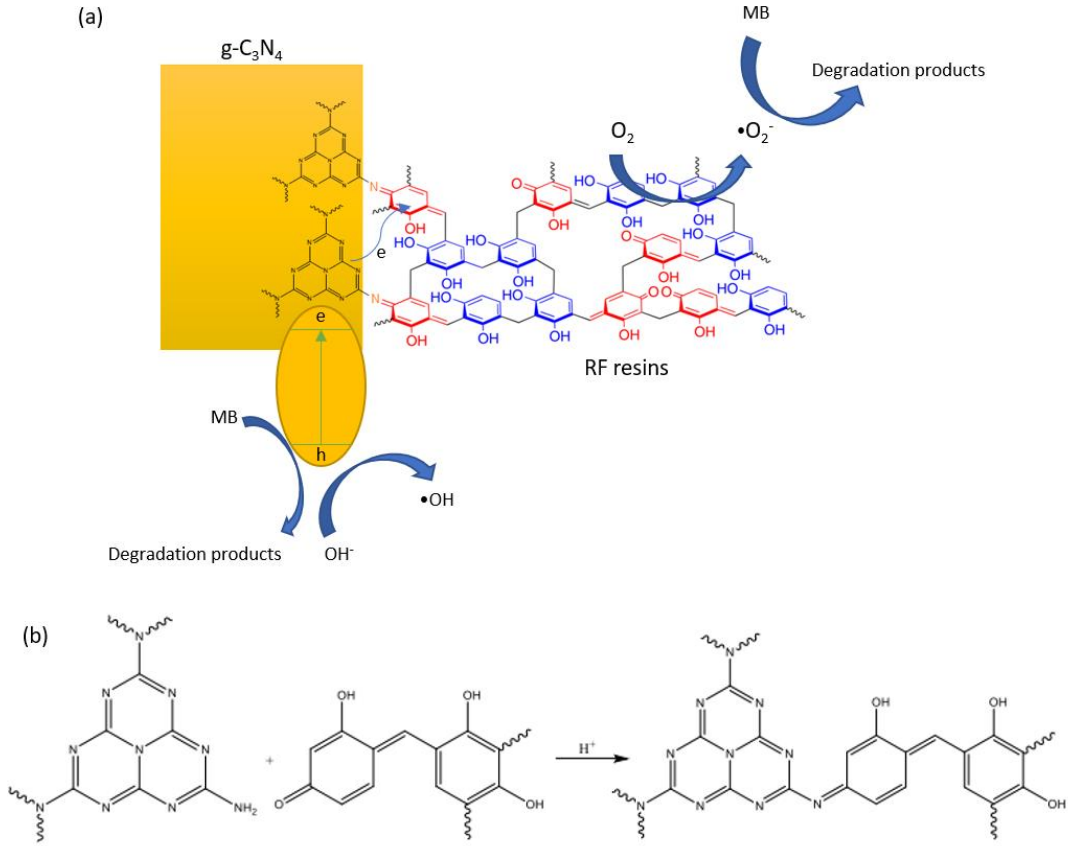

Figure 10: Proposed mechanism of (a) the degradation of MB by RF@CN photocatalyst and (b) the crosslinking between RF resins and carbon nitride

https://doi.org/10.51316/jca.2023.004

In this part of the study, the formation of RF@CN composites is discussed. We conducted a RF@CN material synthesis in which the acidic refluxing step was skipped. The resulting material had light yellow color resembling pristine CN, indicating that RF could not bind on the surface of carbon nitride in basic conditions. In other words, RF can form a bond with carbon nitride in acidic conditions. In order to propose the formation mechanism of RF@CN composite materials, it is necessary to consider the structure of each material. For RF resins, there are quinoid groups that are capable of reacting with a variety of nucleophiles to create crosslinks [22].

Meanwhile, carbon nitride possesses primary and/or secondary amine groups on the terminating edges of the single-layers [23]. It has been proposed that amines could react with the C=O group in quinones via either Michael addition or Schiff base reaction [22]. Due to the bulky structure of carbon nitride, the reaction of amines with quinones is more likely to follow the Schiff base pathway, which formed C=N bridges.

Therefore, we proposed a hypothesis that C=N bridges contribute to the crosslinking of the carbon nitride with RF-resin fragments (Figure 10b). This leads to the extension of π-conjugate system, and the reduction of electron recombination rate, therefore, the photocatalytic performance of the composite is enhanced significantly.

Conclusion

In this study, our aim was to enhance the photocatalytic performance of carbon nitride by modifying Resorcinol-Formaldehyde resins into the pores and the surface of Carbon nitride. SEM images revealed that RF resins appeared as nano-fragments and were deposited densely on the surface of carbon nitride. On the other hand, the deposition of RF on the surface of carbon nitride did not have a great influence on the BET surface area values. The modification step was conducted via solvothermal reflux at 120°C, and the length of the polymerization reaction had a great impact on the photocatalytic activity of the as-prepared samples. All the modified samples exhibited significantly improved photocatalytic activity towards MB. The optimal sample was RF@CN10, which the reflux time was 10 hours. This sample has a more broaden absorption spectrum and a narrower bandgap energy (2.66 eV) than the pure carbon nitride. With regard to photocatalytic activity, this sample could completely degrade MB in the solution within 40 minutes, but it had poor efficiency when visible light was absent. Additionally, the catalyst could work effectively in neutral and alkaline conditions and could be reused for 5 cycles. Finally, the hypothesis for RF-carbon nitride cross-linking and the synergistic effect in the catalyst had been proposed.

Acknowledgments

This research was funded by Vingroup Joint Stock Company and supported by the Domestic Master/ PhD Scholarship Programme of Vingroup Innovation Foundation (VINIF), Vingroup Big Data Institute (VINBIGDATA), code 2020.ThS49.

References

1. C. Li, Y. Xu, W. Tu, G. Chen, R. Xu, Green Chemistry 19 (2017) 882. https://10.1039/c6gc02856j
2. G.O. Hartley, N. Martsinovich, Faraday Discussions 227 (2021) 341. https://10.1039/C9FD00147F
3. B. Karaca, Y. Karataş, A.B. Cakar, M. Gülcan, F. Şen, in: S. Thomas, P. Balakrishnan (Eds.), Nanoscale Processing, Elsevier, 2021, p. 103.
4. X. Wang, K. Maeda, A. Thomas, K. Takanabe, G. Xin, J.M. Carlsson, K. Domen, M. Antonietti, Nature Materials 8 (2009) 76. https://10.1038/nmat2317
5. Y. Kumar, S. Rani, J. Shabir, L.S. Kumar, ACS Omega 5 (2020) 13250. https://10.1021/acsomega.0c01280
6. Q. Liu, H. Tian, Z. Dai, H. Sun, J. Liu, Z. Ao, S. Wang, C. Han, S. Liu, Nanomicro Lett 12 (2020) 24. https://10.1007/s40820-019-0358-x
7. J. Lin, W. Tian, H. Zhang, X. Duan, H. Sun, S. Wang, Energy & Fuels 35 (2021) 7. https://10.1021/acs.energyfuels.0c03048
8. N.S. Heo, S. Shukla, S.Y. Oh, V.K. Bajpai, S.U. Lee, H.-J. Cho, S. Kim, Y. Kim, H.J. Kim, S.Y. Lee, Y.-S. Jun, M.-H. Oh, Y.-K. Han, S.M. Yoo, Y.S. Huh, Materials Science and Engineering: C 104 (2019) 109846. https://doi.org/10.1016/j.msec.2019.109846
9. Y. Luo, Y. Yan, S. Zheng, H. Xue, H. Pang, Journal of Materials Chemistry A 7 (2019) 901. https://10.1039/c8ta08464e

10. J.A. Brydson, in: J.A. Brydson (Ed.), Plastics Materials (Seventh Edition), Butterworth-Heinemann, Oxford, 1999, p. 635.
11. Y. Shiraishi, T. Takii, T. Hagi, S. Mori, Y. Kofuji, Y. Kitagawa, S. Tanaka, S. Ichikawa, T. Hirai, Nat Mater 18 (2019) 985. https://10.1038/s41563-019-0398-0
12. M.T. Islam, C. Hernandez, M.A. Ahsan, A. Pardo, H. Wang, J.C. Noveron, Journal of Environmental Chemical Engineering 5 (2017) 5270. https://10.1016/j.jece.2017.10.003
13. J. Liu, S.Z. Qiao, H. Liu, J. Chen, A. Orpe, D. Zhao, G.Q. Lu, Angew Chem Int Ed Engl 50 (2011) 5947. https://10.1002/anie.201102011
14. X. She, H. Xu, Y. Xu, J. Yan, J. Xia, L. Xu, Y. Song, Y. Jiang, Q. Zhang, H. Li, Journal of Materials Chemistry A 2 (2014). https://10.1039/c3ta13768f
15. S.P. Pattnaik, A. Behera, S. Martha, R. Acharya, K. Parida, Journal of Materials Science 54 (2019) 5726. https://10.1007/s10853-018-03266-x
16. D.R. Paul, R. Sharma, S.P. Nehra, A. Sharma, RSC Advances 9 (2019) 15381. https://10.1039/C9RA02201E
17. X. Wang, D. Li, Z. Nan, Separation and Purification Technology 224 (2019) 152. https://doi.org/10.1016/j.seppur.2019.04.088
18. B. Lin, G. Yang, B. Yang, Y. Zhao, Applied Catalysis B: Environmental 198 (2016) 276. https://doi.org/10.1016/j.apcatb.2016.05.069
19. L. Ge, C. Han, J. Liu, Journal of Materials Chemistry 22 (2012) 11843. https://10.1039/C2JM16241E
20. S. Munusamy, K. Sivaranjan, P. Sabhapathy, V. Narayanan, F. Mohammad, S. Sagadevan, Synthetic Metals 272 (2021) 116669. https://doi.org/10.1016/j.synthmet.2020.116669
21. G. Zhang, C. Ni, L. Liu, G. Zhao, F. Fina, J.T.S. Irvine, Journal of Materials Chemistry A 3 (2015) 15413. https://10.1039/c5ta03628c
22. J. Yang, V. Saggiomo, A.H. Velders, M.A. Cohen Stuart, M. Kamperman, PLoS One 11 (2016) https://e0166490. 10.1371/journal.pone.0166490
23. J. Wen, J. Xie, X. Chen, X. Li, Applied Surface Science 391 (2017) 72. https://doi.org/10.1016/j.apsusc.2016.07.030